12th International Symposium on Turbulence and Shear Flow Phenomena (TSFP12)
Osaka, Japan (Online), July 19-22, 2022

SPECTRAL BEHAVIOR OF SELF-SIMILAR COHERENT STRUCTURES IN CANONICAL WALL-BOUNDED TURBULENT FLOWS

Jinyul Hwang
School of Mechanical Engineering
Pusan National University
Busan 46241, Korea
jhwang@pusan.ac.kr

Jae Hwa Lee
Department of Mechanical Engineering
UNIST
Ulsan 44919, Korea
jhlee06@unist.ac.kr

Hyung Jin Sung
Department of Mechanical Engineering
KAIST
Daejeon 34141, Korea
hjsung@kaist.ac.kr

ABSTRACT

The attached-eddy hypothesis (AEH) conjectured by Townsend (1976) predicts asymptotic behaviours of turbulence statistics in the logarithmic region in terms of self-similar coherent motions, yet revealing such behaviours has remained an elusive task because the proposed description is established within the limits of asymptotically high Reynolds numbers. In the present work, we scrutinized the self-similar behaviour of turbulence motions contained within wall-attached structures of streamwise velocity fluctuations (u) using the direct numerical simulation dataset of turbulent boundary layer, channel, and pipe flows ($Re_\tau \approx 1000$). The physical sizes of the identified structures across the logarithmic region are geometrically self-similar in terms of height. In addition, the two-dimensional energy spectra of u within the self-similar structures follow a linear relationship between the streamwise and spanwise wavelengths in the large-scale range, which is reminiscent of self-similarity. The present results revealed that the asymptotic behaviors can be captured by extracting the self-similar coherent motions in canonical wall turbulence, even at relatively low-Reynolds-number flows. More details can be found in Hwang *et al.* (2020).

INTRODUCTION

Wall turbulence is characterized by a broad range of scales, from the viscous length scale (δ_v) to the outer length scale (δ). The friction Reynolds number ($Re_\tau = \delta/\delta_v$) describes such a multiscale phenomena. At extremely high Re_τ, there is a region that is sufficiently far from the wall and far from the outer region. This region is the so-called logarithmic region where the only relevant length scale is the distance from the wall y, and the mean velocity profile follows the logarithmic variation with respect to y (Millikan, 1938). Townsend (1976) hypothesized that coherent motions in the logarithmic region are self-similar and that their sizes are proportional to y. Townsend's hypothesis was further extended by Perry & Chong (1982), who deduced the attached-eddy model. Based on the attached-eddy model, they expected that the logarithmic variations occur in the mean velocity and in the wall-parallel components of turbulence intensity. The model also shows that self-similar motions contribute to a k_x^{-1} scaling in the one-dimensional spectra of the streamwise velocity, where k_x is the streamwise wavenumber. The k_x^{-1} region was predicted by Perry & Abell (1977), who assumed that there is a spectral overlap region where y and δ scalings hold simultaneously. In this sense, the k_x^{-1} region can be a consequence of the AEH and is deemed the spectral signature of attached eddies (Perry & Chong, 1982; Perry *et al.*, 1986). However, although some studies have shown empirical evidence for the existence of the k_x^{-1} region (Nickels *et al.*, 2005; Vallikivi *et al.*, 2015), it remains unclear whether such scaling exists in a high-Reynolds-number flow (Rosenberg *et al.*, 2013; Lee & Moser, 2015; Ahn *et al.*, 2015; Agostini & Leschziner, 2017; Chandran *et al.*, 2017; Baars & Marusic, 2020).

The ambiguities in the spectral signatures of the attached eddies are related to insufficient scale separation because the AEH requires that the Reynolds number approaches infinity. This means no region exists in which both y and δ scalings are valid over the same wavenumber space, even in the high-Reynolds-number experiments $Re = O(10^{4-5})$ of the aforementioned studies. However, given the fact that the self-similar energy-containing motions follow a hierarchical distribution (Perry & Chong, 1982), we may expect that self-similar motions can exist even if scale separation is insufficient. Owing to insufficient separation of scales, self-similar motions are less statistically dominant than other coexisting motions, which in turn leads to ambiguity of the asymptotic behaviours in turbulent statistics.

Recently, Hwang & Sung (2018) extracted the wall-attached structures of the streamwise velocity fluctuations (u) in turbulent boundary layer (TBL) and found that the identified structures were self-similar in terms of their heights (l_y), directly contributing to the logarithmic variation in the streamwise turbulence intensity. In addition, they showed that the population density of the identified structures was inversely proportional to l_y, reminiscent of the hierarchies of self-similar eddies (Townsend, 1976; Perry & Chong, 1982). Moreover, in pipe flows, the profile of the streamwise velocity reconstructed by the superposition of the wall-attached u structures exhibits

the logarithmic variation (Hwang & Sung, 2019). Despite evidence on the self-similarity of wall-attached u structures and their contribution to the logarithmic behaviors, their spectral contributions and the turbulence motions contained within the identified structures have not been revealed. Because the wall-attached u structures are identified in instantaneous fluctuating velocity fields, a wide range of scales is contained within the individual structure. Therefore, spectral analysis is required to reveal whether the large scales contained within the identified object can be attributed to the logarithmic variation or exhibit the spectral overlap argument proposed by Perry and coworkers (Perry & Chong, 1982).

The objective of the present study is to explore the spectral contribution of turbulence motions that comprise wall-attached u clusters by computing the two-dimensional spectra of u, in which the velocity signals contained within self-similar structures are isolated. We examined the direct numerical simulation (DNS) data of a fully developed turbulent channel and pipe flows, along with zero-pressure-gradient TBL at $Re_\tau \approx 1000$, and identify the wall-attached self-similar structures by applying universal filters in terms of height. The wall-attached u clusters were decomposed into the buffer-layer, self-similar, and non-self-similar structures in terms of their height. The wall-attached self-similar structures were further examined using the two-dimensional energy spectra to reveal the self-similar behaviours in the logarithmic region of all three flows. We then explored the one-dimensional streamwise and spanwise spectra by comparing the energy contained in the spectral range where the energetic ridges in the two-dimensional spectra follow a linear relationship between the wall-parallel wavelengths.

NUMERICAL DETAILS

In this study, we analysed the DNS data of the zero-pressure gradient TBL (Hwang & Sung, 2017; Yoon *et al.*, 2018) as well as the fully developed turbulent channel (Lee *et al.*, 2014, 2015) and pipe flows (Ahn *et al.*, 2013, 2015). A detailed description of the DNS can be found in the aforementioned studies. The friction Reynolds numbers, defined as the ratio of the outer length scale to the viscous length scale, match at $Re_\tau = u_\tau \delta/\nu \approx 1000$. Here, u_τ is the friction velocity, ν is the kinematic velocity, and δ is the flow thickness (i.e. channel half-height, pipe radius, or 99% boundary layer thickness). Throughout the present work, the superscript $+$ represents viscous scaling (ν/u_τ and u_τ). In the present study, x, y, and z indicate the streamwise, wall-normal, and spanwise directions, respectively. In the pipe flow, the wall-normal direction is defined as $y = \delta - r$, where r denotes the radial direction. In addition, for an analogy with z in the TBL and channel flows, the spanwise dimension of the pipe is defined as the arclength $r\theta$, where θ denotes the azimuthal direction. We define the streamwise velocity fluctuations $u = U - \overline{U}(y)$, where U is the streamwise velocity, and the overbar denotes the ensemble average.

We identified the clusters of u in the instantaneous flow fields by extracting the contiguous points of the intense u region (Hwang & Sung, 2018, 2019; Han *et al.*, 2019; Yoon *et al.*, 2020). In the three-dimensional flow field, the irregular shapes of the objects are defined as

$$u(x,y,z) > \alpha u_{rms}(y) \text{ or } u(x,y,z) > -\alpha u_{rms}(y), \qquad (1)$$

where u_{rms} is the standard deviation of the streamwise velocity and α is the threshold. Individual objects are extracted using the connectivity rule, in which nodes are labelled among the six orthogonal neighbours of each node satisfying (1) in Cartesian coordinates (Moisy & Jiménez, 2004; del Álamo *et al.*, 2006; Lozano-Durán *et al.*, 2012; Hwang & Sung, 2018) and cylindrical coordinates (Hwang & Sung, 2019; Han *et al.*, 2019). We chose the threshold $\alpha = 1.5$ for all three flows; further discussion can be found in our previous works (Hwang & Sung, 2018; Yoon *et al.*, 2020). The present identification method allows us to measure the physical length scales of individual structures in instantaneous flow fields. Each structure is bounded by a box of size $l_x \times l_y \times l_z$, where the corresponding length, height, and width are denoted by l_x, l_y, and l_z. In the pipe flow, l_z is computed in terms of the maximum arc length in the plane obtained by projecting each object onto the cross-stream plane.

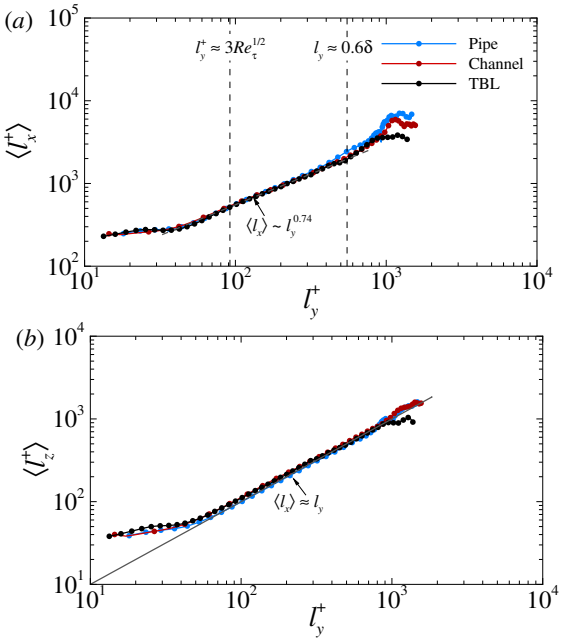

Figure 1. The size distributions of wall-attached u structures. (a) Mean length ($\langle l_x \rangle$) with respect to l_y. (b) Mean width ($\langle l_z \rangle$) with respect to l_y.

RESULTS AND DISCUSSION

To extract the wall-attached self-similar structures (WASS), we examined the mean streamwise length $\langle l_x \rangle$ and the mean spanwise width $\langle l_z \rangle$ at a given l_y (figure 1). In figure 1(a), we can see a power-law behavior (i.e. $\langle l_x \rangle \sim l_y^{0.74}$) over $3Re_\tau^{1/2} < l_y{}^+ < 0.6\delta^+$ (figure 1a) in all three flows. On the other hand, for the width of the identified structures (figure 1b), the linear relationship is observed; i.e., $\langle l_z \rangle \sim l_y$ over $l_y^+ > 3Re_\tau^{1/2}$. Although no linear relationship exists for the wall-attached u structures over $3Re_\tau^{1/2} \le l_y^+ < 0.6\delta^+$ in figure 1(a), the sizes of the structures are scaled with l_y and show a good agreement regardless of flow geometry. According to figure 1, we classified the wall-attached u structures as three components in terms of l_y: buffer-layer structures, self-similar structures, and non-self-similar structures, defined as $l_y^+ < 3Re_\tau^{1/2}$, $3Re_\tau^{1/2} \le l_y^+ < 0.6\delta^+$, and $0.6\delta \le l_y^+$, respectively. Here, the lower bound ($= 3Re_\tau^{1/2}$) of self-similar structures corresponds to that of the logarithmic region in Marusic *et al.* (2013) and Hwang & Sung (2019). The present Reynolds

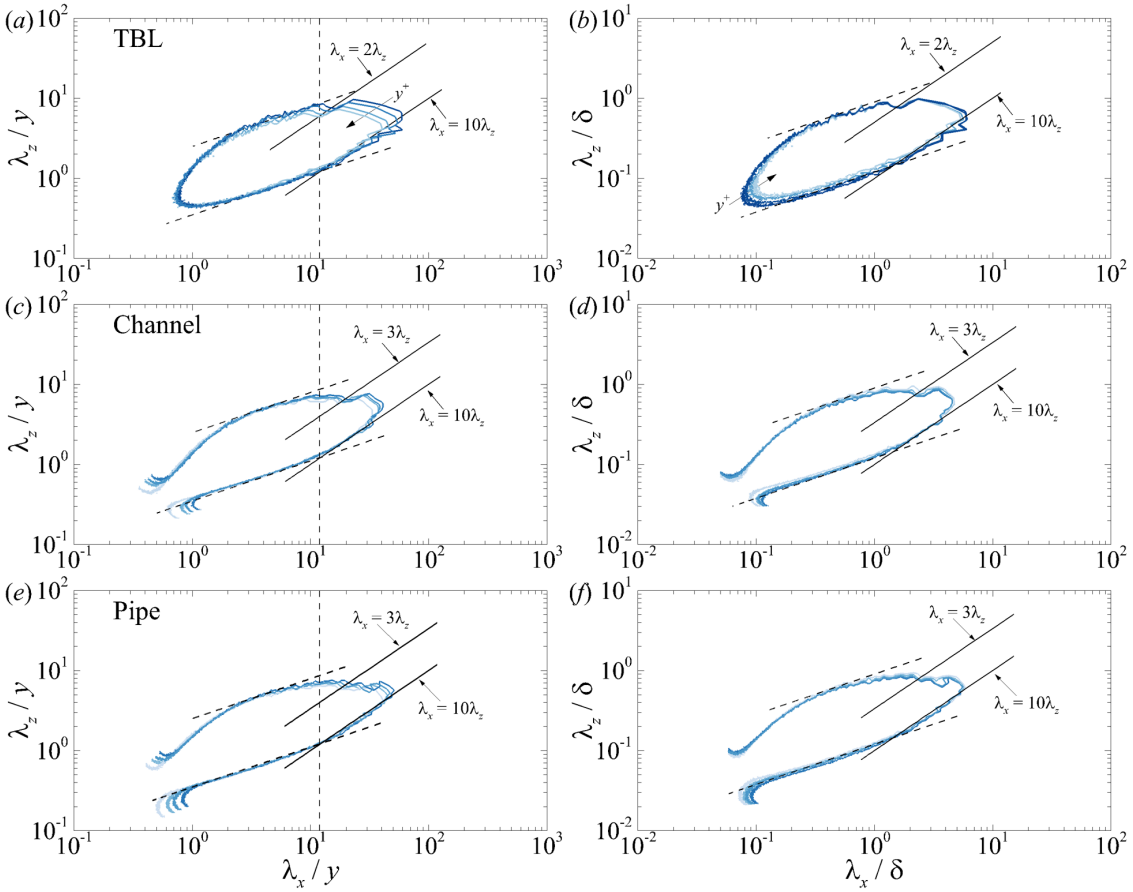

Figure 2. Premultiplied two-dimensional energy spectra Φ^{2D} at $y^+ = 100, 110, 120$, and 130: (a,b) TBL, (c,d) channel, and (e,f) pipe. Dark to light shading indicates an increase in y. The contour level is 0.4 times each of the maxima. The dashed and solid lines denote $\lambda_x/y \sim (\lambda_z/y)^2$ and $\lambda_x \sim \lambda_z$, respectively. The vertical dashed line in the left column indicates $\lambda_x = 12y$.

number is $Re_\tau \approx 1000$; therefore, the lower bound of the logarithmic region is approximately 100 wall units ($3Re_\tau^{1/2} \approx 100$), that is, a classical scaling for the lower bound of the logarithmic region (Perry & Chong, 1982).

Next, we conditionally sampled u signals contained within the bounded volume of each WASS in instantaneous flow field (u_{ws}) to examine the spectral contributions of various scales associated within the WASS. The u signals outside the WASS are artifically imposed to zero (Lee *et al.*, 2015; Hwang *et al.*, 2016*b*, 2020). The contribution of coherent motions ingrained within WASS to the streamwise variance is explored by computing the premultiplied two-dimensional spectrum of u_{ws} (figure 2).

$$\Phi^{2D}(k_x,k_z,y) = k_x k_z \langle \hat{u}_{ws}(k_x,k_z,y)\hat{u}^*_{ws}(k_x,k_z,y)\rangle, \qquad (2)$$

where $k_x(=2\pi/\lambda_x)$ and $k_z(=2\pi/\lambda_z)$ are the streamwise and spanwise wavenumbers, and $\hat{u}_{ws}$ indicates the Fourier coefficient of u_{ws} and the asterisk denotes a complex conjugate.

In general, all three flows show that Φ^{2D} scales reasonably well with y in the range $y < \lambda_x < 10y$ (figure $2a,c,e$) and with δ in the range $\lambda_x > \delta$ (figure $2b,d,f$). In particular, the bounds of the constant energy distribution are aligned along a linear relationship between the streamwise and spanwise wavelengths (λ_x and λ_z, respectively) in the large-scale range ($12y < \lambda_x < 3$–4δ). This spectral feature is found in all three flows indicative of the universality of the self-similar nature of the large scales contained within WASSs. In addition, $\lambda_x > 12y$ is consistent with the lower limit of the k_x^{-1} region in channel flows (Hwang, 2015), and is close to the inner-scaling limit ($\lambda_x = 14y$) of self-similar motions in TBLs over a wide range of Re_τ (Baars *et al.*, 2017). Deshpande *et al.* (2020) also found the existence of linear behaviour in two-dimensional cross spectra of wall-coherent u motions over a similar range (i.e. $\lambda_x > 15y$). This shows that the WASS identified in the present study is directly related to the self-similar behaviour in the wavenumber space.

However, the wall-attached u structures defined in the present study (Eq.(1)) depend on the threshold value α because we identified the structures by extracting the physically connected volumes of intense fluctuations. Therefore, we examined the influence of the threshold value over a certain range in the vicinity of $\alpha \approx 1.5$. The threshold effect on the population density and the sizes of the bounding box was reported in Hwang & Sung (2018, 2019). Figure 3 shows the effect of α on (Φ^{2D}. Here, we plot Φ^{2D} for TBL only to avoid any repetition. We can see that all the contours collapse reasonably well regardless of α. In particular, the linear relationship (λ_x λ_z) appears at $\lambda_x > 12y$, and the lower bounds align along $\lambda_x = 10\lambda_z$ regardless of the threshold. This result shows that the conditionally sampled flow field u_{ws} can represent a continuous range of scales related to the energy-containing motions in the logarithmic region.

Figure 4 shows the spectral ridge of Φ^{2D}. We determined the spectral ridge by identifying λ_z, where the maximum value of Φ^{2D} occurs at a given λ_x. As seen, the spectral ridges are found to agree reasonably well over a wide range of scales.

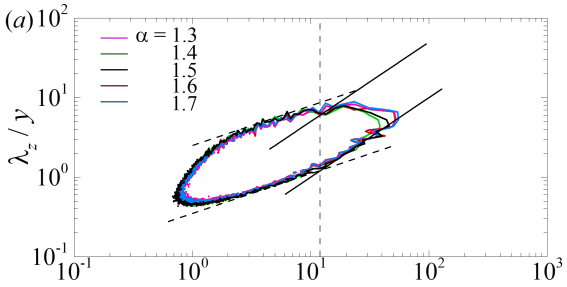

Figure 3. Premultiplied two-dimensional energy spectra Φ^{2D} at $y^+ = 120$ in TBL with $\alpha = 1.3, 1.4, 1.5, 1.6$, and 1.7. The dashed and solid lines are consistent with those in figure 2(a). The vertical dashed line indicates $\lambda_x = 12y$.

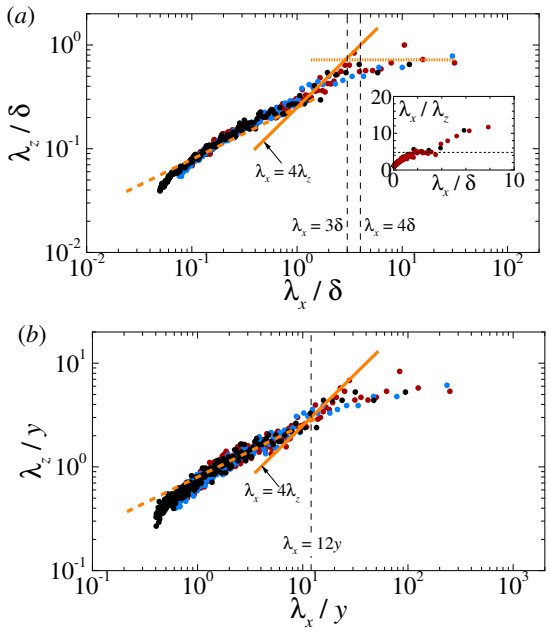

Figure 4. Energetic ridges of the premultiplied two-dimensional energy spectra Φ^{2D} at $y^+ = 120$. In (a), the inset shows the lin-lin plot of the ridge scale ratio λ_x/λ_z for the TBL and channel data. The horizontal dashed line denotes a constant ratio $\lambda_x/\lambda_z \approx 4$.

In particular, we observed two growth rates, the power-law behaviour $\lambda_x \sim \lambda_z^2$ (dashed line), and the linear relationship $\lambda_x \sim \lambda_z$ (solid line), at relatively large scales. The transition of the ridges from the power law to the linear law appears at $\lambda_x = 12y$. This result is consistent with the variation of the lower and upper bounds of Φ^{2D} found in figure 2. The spectral ridges become flatten for $\lambda_x > 3-4\delta$ because at this very long λ_x, the spanwise wavelength λ_z reaches δ and the growth of λ_z is restricted.

In figure 4, the linear behaviour seems to follow $\lambda_x \approx 4\lambda_z$ over the range $12y < \lambda_x < 3-4\delta$. Here, the inset shows the ridge scale ratio λ_x/λ_z for the TBL and channel data. A plateau of $\lambda_x/\lambda_z \approx 4$ is clear, indicating the linear relationship. Therefore, the range of the self-similar energetic motions ingrained in WASS can be expressed as

$$12y < \lambda_x < 3-4\delta,\ 3y < \lambda_z < 0.8-1\delta. \qquad (3)$$

Here, the upper limit for the streamwise wavelength in Eq. (3) is $3-4\delta$, similar to that of the criteria that distinguish large-scale motions and very-large-scale motions (Guala *et al.*, 2006; Wu *et al.*, 2012; Hwang *et al.*, 2016*a*). Given that the contours of Φ^{2D} are restricted to below $\lambda_x \approx 3-4\delta$ in figure 2, this result also shows that Φ^{2D} comprises the contribution from the turbulence motions that include large-scale motions and relatively smaller motions. According to Deshpande *et al.* (2020), the two-dimensional spectra of wall-coherent motions at $Re_\tau \approx 15000$ are aligned along a linear ridge $\lambda_x = 7\lambda_z$, which is slightly steeper than the proportionality $\lambda_x = 4\lambda_z$ found in the present work. However, the spectra reported by Deshpande *et al.* (2020) includes the contributions from wall-attached self-similar and non-self-similar motions. Given that very large scales can contaminate self-similar behaviours of turbulent motions (Jiménez & Hoyas, 2008; Hwang & Sung, 2018; Han *et al.*, 2019), it would be instructive in future efforts to examine the energetic ridges of Φ^{2D} over a wide range of Re_τ.

CONCLUSIONS

We explored the wall-attached self-similar structures (WASS) of u from the viewpoint of Townsend's AEH, with special focus on the spectral contribution of turbulence motions contained within the identified structures. We extracted the wall-attached structures of u in the DNS data of a zero-pressure-gradient TBL, and turbulent channel and pipe flows at $Re_\tau \approx 1000$ by extracting the intense u regions across the instantaneous flow fields. Then, the wall-attached structures of u are classified as buffer-layer, self-similar, and non-self-similar structures with respect to the height (l_y). The variations in the physical sizes of WASS show a good agreement in all three flows as well as scale with l_y. We also examined the two-dimensional spectra of u within WASS to explore the spectral signatures of self-similarity. Across the logarithmic region, we found that the lower and upper bounds of the two-dimensional spectra follow a linear relationship $\lambda_x \sim \lambda_z$ in the large-scale range ($\lambda_x > 12y$). Moreover, the spectral ridges exhibit $\lambda_x \approx 4\lambda_z$ over the range $12y < \lambda_x < 3-4\delta$, showing that only the large scales contained in WASS are self-similar. Our results indicate that we can capture the asymptotic behaviours of turbulent statistics, predicted by the AEH, when we adequately filter out contributions from coexisting non-self-similar motions.

ACKNOWLEDGEMENTS

This work was supported by the National Research Foundation of Korea (NRF) grant funded by the Korea government (MSIT) (No. 2020R1F1A1048537) and partially supported by the Supercomputing Center (KISTI).

REFERENCES

Agostini, L. & Leschziner, M. 2017 Spectral analysis of near-wall turbulence in channel flow at $Re_\tau = 4200$ with emphasis on the attached-eddy hypothesis. *Phys. Fluids* **2** (1), 014603.

Ahn, J., Lee, J. H., Jang, S. J. & Sung, H. J. 2013 Direct numerical simulations of fully developed turbulent pipe flows for Re_τ= 180, 544 and 934. *Intl J. Heat Fluid Flow* **44**, 222–228.

Ahn, J., Lee, J. H., Lee, J., Kang, J.-H & Sung, H. J. 2015

Direct numerical simulation of a 30R long turbulent pipe flow at Re_τ= 3008. *Phys. Fluids* **27** (6), 065110.

del Álamo, J. C., Jiménez, J., Zandonade, P. & Moser, R. D. 2006 Self-similar vortex clusters in the turbulent logarithmic region. *J. Fluid Mech.* **561**, 329–358.

Baars, W. J., Hutchins, N. & Marusic, I. 2017 Self-similarity of wall-attached turbulence in boundary layers. *J. Fluid Mech.* **823**.

Baars, W. J. & Marusic, I. 2020 Data-driven decomposition of the streamwise turbulence kinetic energy in boundary layers. part 1. energy spectra. *J. Fluid Mech.* **882**.

Chandran, D., Baidya, R., Monty, J. P. & Marusic, I. 2017 Two-dimensional energy spectra in high-reynolds-number turbulent boundary layers. *J. Fluid Mech.* **826**.

Deshpande, R., Chandran, D., Monty, J. P. & Marusic, I. 2020 Two-dimensional cross-spectrum of the streamwise velocity in turbulent boundary layers. *J. Fluid Mech.* **890**.

Guala, M., Hommema, S. E. & Adrian, R. J. 2006 Large-scale and very-large-scale motions in turbulent pipe flow. *J. Fluid Mech.* **554**, 521–542.

Han, J., Hwang, J., Yoon, M., Ahn, J. & Sung, H. J. 2019 Azimuthal organization of large-scale motions in a turbulent minimal pipe flow. *Phys. Fluids* **31** (5), 055113.

Hwang, J., Lee, J. & Sung, H. J. 2016*a* Influence of large-scale accelerating motions on turbulent pipe and channel flows. *J. Fluid Mech.* **804**, 420–441.

Hwang, J., Lee, J., Sung, H. J. & Zaki, T. A. 2016*b* Inner-outer interactions of large-scale structures in turbulent channel flow. *J. Fluid Mech.* **790**, 128–157.

Hwang, J., Lee, J. H. & Sung, H. J. 2020 Statistical behaviour of self-similar structures in canonical wall turbulence. *J. Fluid Mech.* **905**.

Hwang, J. & Sung, H. J. 2017 Influence of large-scale motions on the frictional drag in a turbulent boundary layer. *J. Fluid Mech.* **829**, 751–779.

Hwang, J. & Sung, H. J. 2018 Wall-attached structures of velocity fluctuations in a turbulent boundary layer. *J. Fluid Mech.* **856**, 958–983.

Hwang, J. & Sung, H. J. 2019 Wall-attached clusters for the logarithmic velocity law in turbulent pipe flow. *Phys. Fluids* **31** (5), 055109.

Hwang, Y. 2015 Statistical structure of self-sustaining attached eddies in turbulent channel flow. *J. Fluid Mech.* **767**, 254–289.

Jiménez, J. & Hoyas, S. 2008 Turbulent fluctuations above the buffer layer of wall-bounded flows. *J. Fluid Mech.* **611**, 215–236.

Lee, J., Ahn, J. & Sung, H. J. 2015 Comparison of large- and very-large-scale motions in turbulent pipe and channel flows. *Phys. Fluids* **27** (2), 025101.

Lee, J., Lee, J. H., Choi, J.-I. & Sung, H. J. 2014 Spatial organization of large-and very-large-scale motions in a turbulent channel flow. *J. Fluid Mech.* **749**, 818–840.

Lee, M. & Moser, R. D. 2015 Direct numerical simulation of turbulent channel flow up to reτ=5200. *J. Fluid Mech.* **774**, 395–415.

Lozano-Durán, A., Flores, O. & Jiménez, J. 2012 The three-dimensional structure of momentum transfer in turbulent channels. *J. Fluid Mech.* **694**, 100–130.

Marusic, I., Monty, J. P., Hultmark, M. & Smits, A. J. 2013 On the logarithmic region in wall turbulence. *J. Fluid Mech.* **716**, R3.

Millikan, C. B. 1938 A critical discussion of turbulent flow in channels and circular tubes. In *Proc. 5th Int. Congress on Applied Mechanics (Cambridge, MA, 1938)*, pp. 386–392. Wiley.

Moisy, F. & Jiménez, J. 2004 Geometry and clustering of intense structures in isotropic turbulence. *J. Fluid Mech.* **513**, 111–133.

Nickels, T. B., Marusic, I., Hafez, S. & Chong, M. S. 2005 Evidence of the k_1^{-1} law in a high-Reynolds-number turbulent boundary layer. *Phys. Rev. Lett.* **95** (7), 074501.

Perry, A. E. & Abell, C. J. 1977 Asymptotic similarity of turbulence structures in smooth-and rough-walled pipes. *J. Fluid Mech.* **79** (4), 785–799.

Perry, A. E. & Chong, M. S. 1982 On the mechanism of wall turbulence. *J. Fluid Mech.* **119**, 173–217.

Perry, A. E., Henbest, S. & Chong, M. S. 1986 A theoretical and experimental study of wall turbulence. *J. Fluid Mech.* **165**, 163–199.

Rosenberg, B. J., Hultmark, M., Vallikivi, M., Bailey, S. C. C. & Smits, A. J. 2013 Turbulence spectra in smooth-and rough-wall pipe flow at extreme reynolds numbers. *J. Fluid Mech.* **731**, 46–63.

Townsend, A. A. 1976 *The structure of turbulent shear flow*. Cambridge university press.

Vallikivi, M., Ganapathisubramani, B. & Smits, A. J. 2015 Spectral scaling in boundary layers and pipes at very high reynolds numbers. *J. Fluid Mech.* **771**, 303–326.

Wu, X., Baltzer, J. R. & Adrian, R. J. 2012 Direct numerical simulation of a 30R long turbulent pipe flow at R^+ = 685: large- and very large-scale motions. *J. Fluid Mech.* **698**, 235–281.

Yoon, M., Hwang, J. & Sung, H. J. 2018 Contribution of large-scale motions to the skin friction in a moderate adverse pressure gradient turbulent boundary layer. *J. Fluid Mech.* **848**, 288–311.

Yoon, M., Hwang, J., Yang, J. & Sung, H. J. 2020 Wall-attached structures of streamwise velocity fluctuations in an adverse-pressure-gradient turbulent boundary layer. *J. Fluid Mech.* **885**.